Supporting Information for "3-D elastic and anelastic structure of the lowermost mantle beneath the western Pacific from finite-frequency tomography"

Kensuke Konishi[1], Nobuaki Fuji[2], and Frédéric Deschamps[1]

[1]Institute of Earth Sciences, Academia Sinica, 128 Academia Road Sec. 2, Nangang, Taipei 11529, Taiwan

[2]Institut de Physique du Globe de Paris, 1 rue Jussieu 75238 Paris Cedex 05

Additional Supporting Information (Files uploaded separately)

1. Captions for Figures S1 to S10

Introduction This supporting information is provided to show robustness of the inversion. Trade-offs between the target region and shallower regions are also examined.

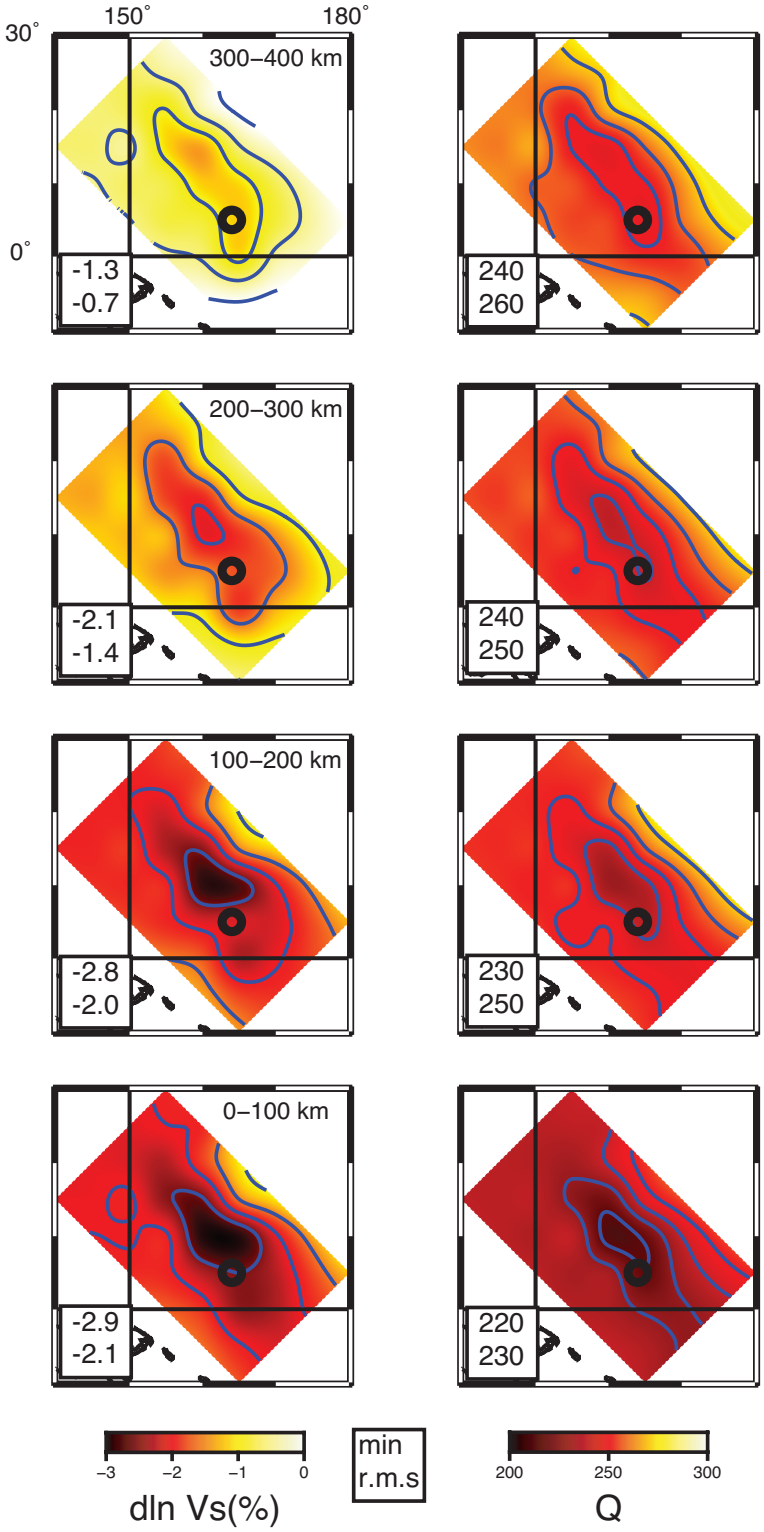

Figure S1. Models obtained with weaker weighting on both $d \ln V_S$ and Q. $a = a_0$, $\gamma = 0.5 \times \gamma_0$, $\xi = \xi_0$, $w_V = w_{V0}$ and $w_q = w_{q0}$. Legends and contour interval are the same as in Fig. 4.

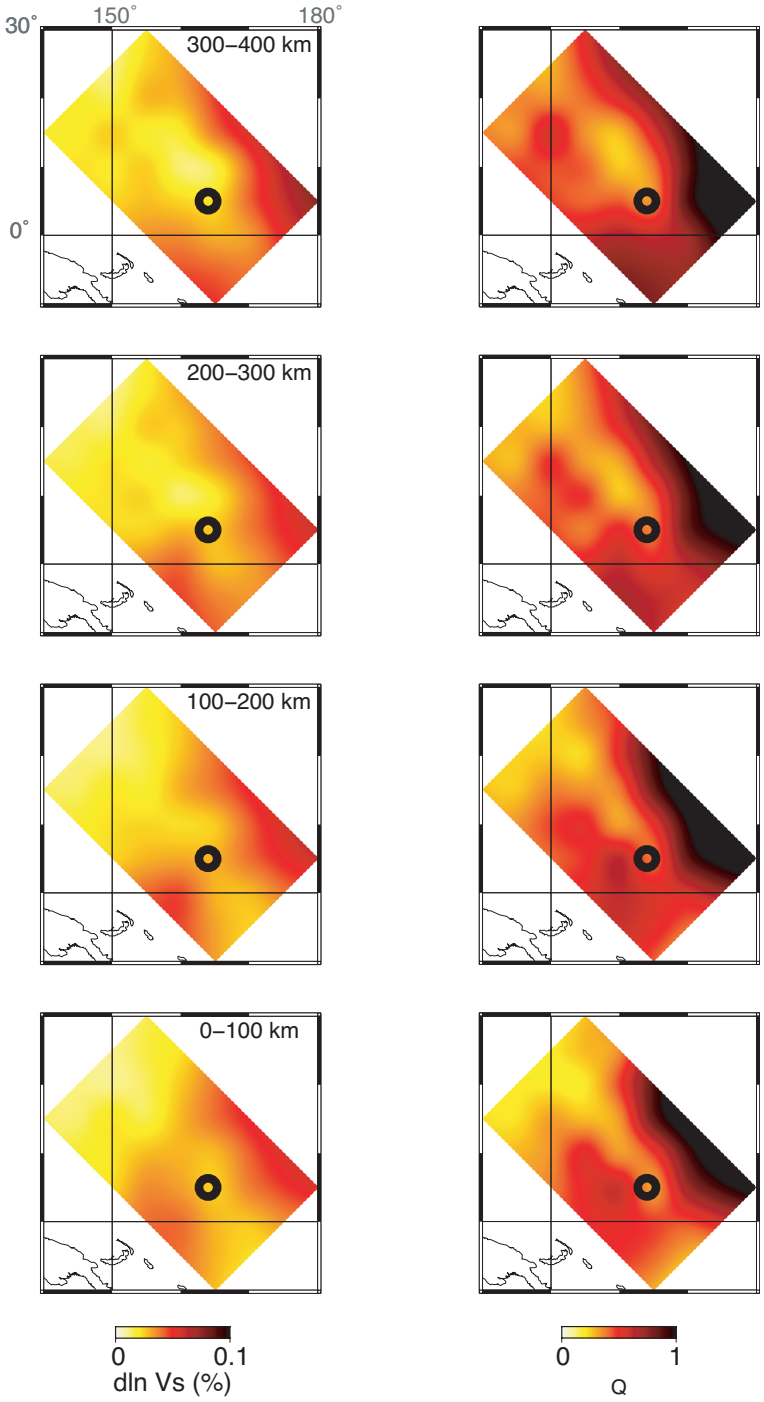

Figure S2. Standard deviation of the differences between the $d \ln V_S$ and Q models obtained from the bootstrap test and our preferred models.

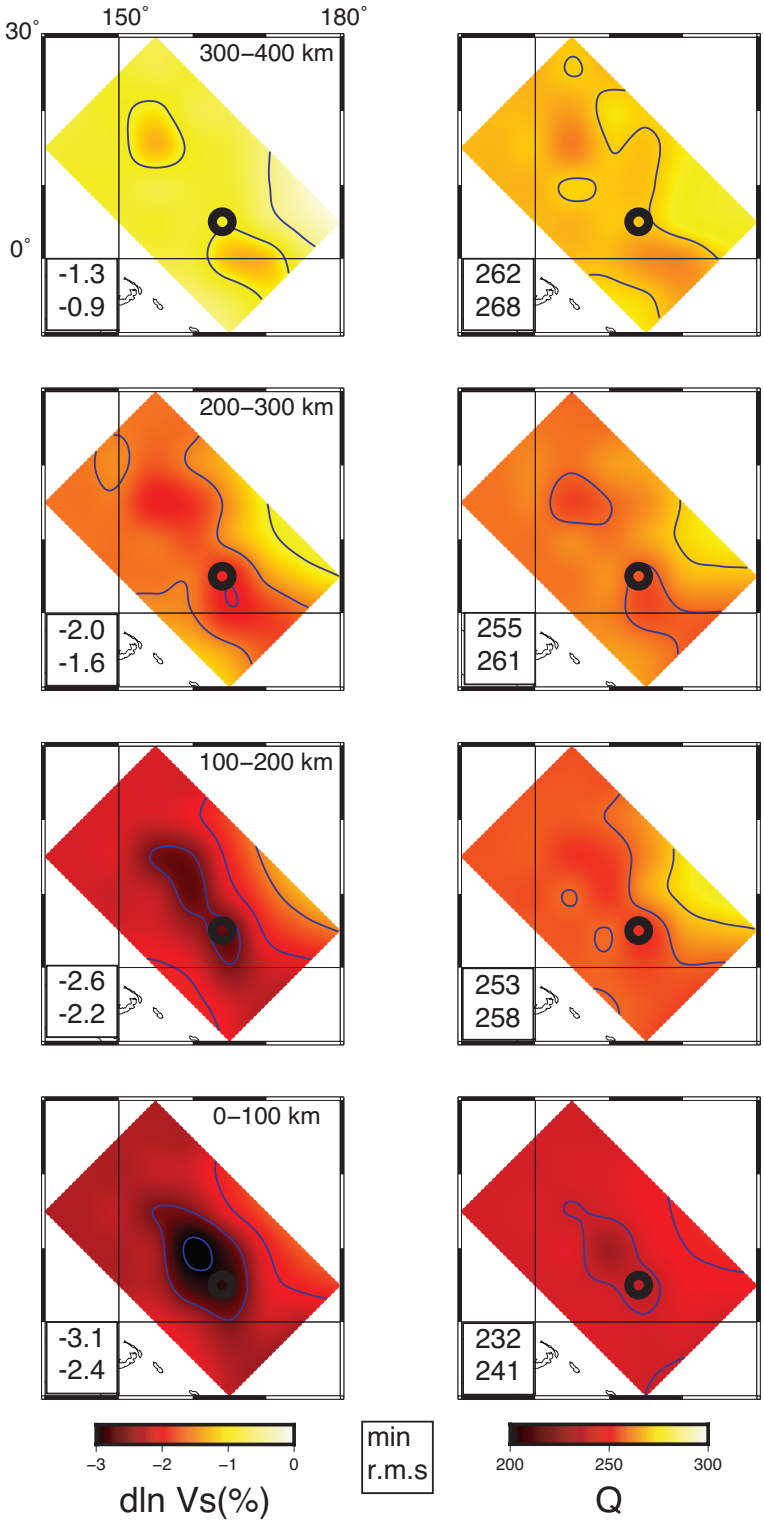

Figure S3. Models obtained using dataset without static correction. Legends and contour interval are the same as in Fig. 4.

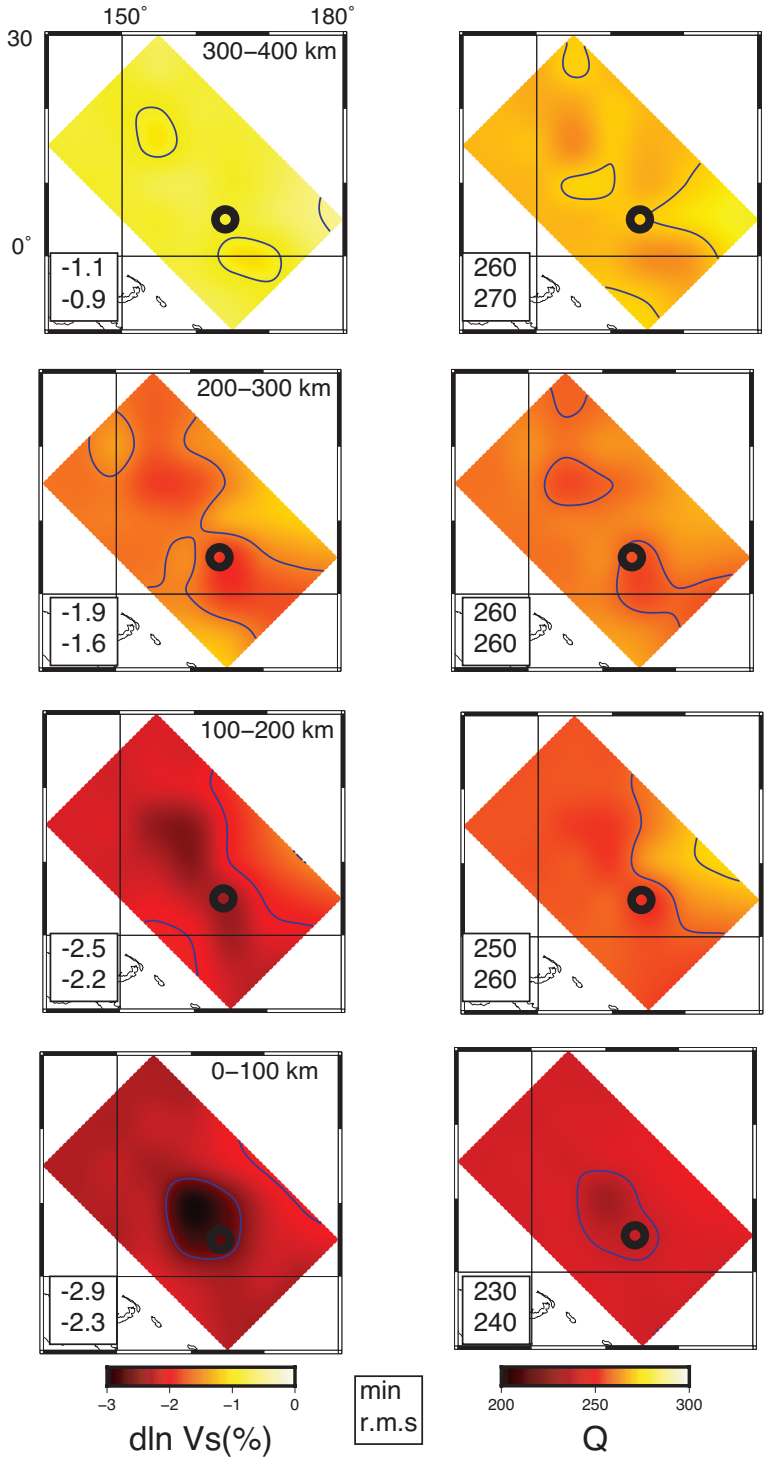

Figure S4. Models obtained with 1-D partial derivatives for shallow depth range and 3-D kernel for the lowermost range. Legends and contour interval are the same as in Fig. 4.

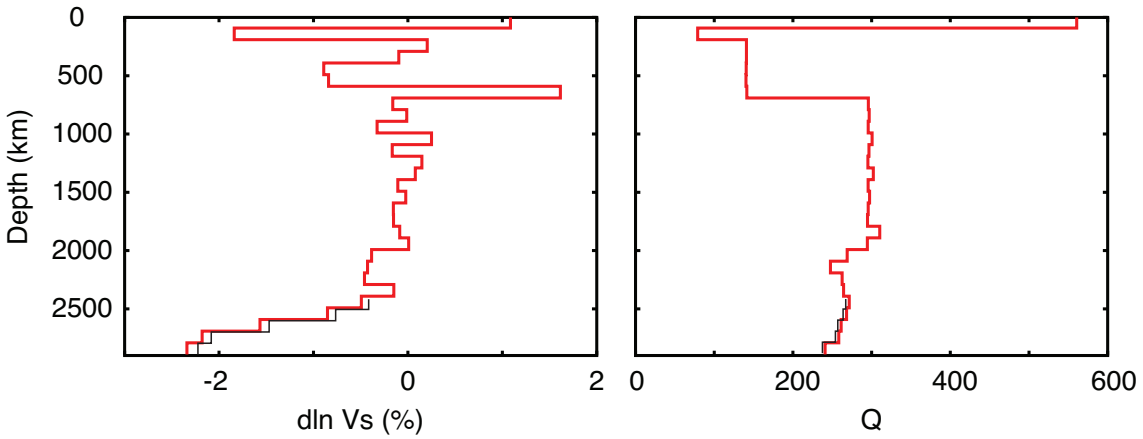

Figure S5. Models obtained with 1-D partial derivatives for shallow depth range and 3-D partial derivatives for the lowermost range (in red). Within a depth range of the lowermost 400 km, the averaged value for each 100 km is plotted. For comparison, the averaged values of the preferred model (Fig. 4) is shown in black.

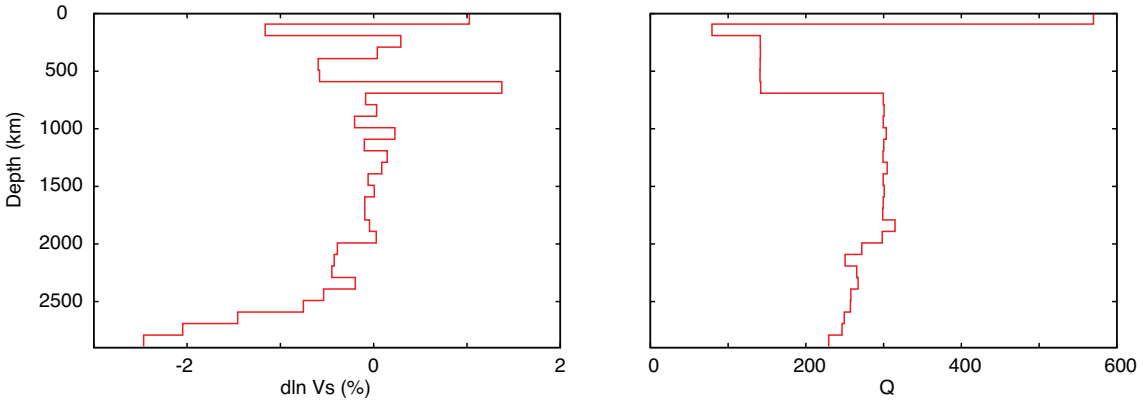

Figure S6. Models obtained with 1-D partial derivatives for entire depth range.

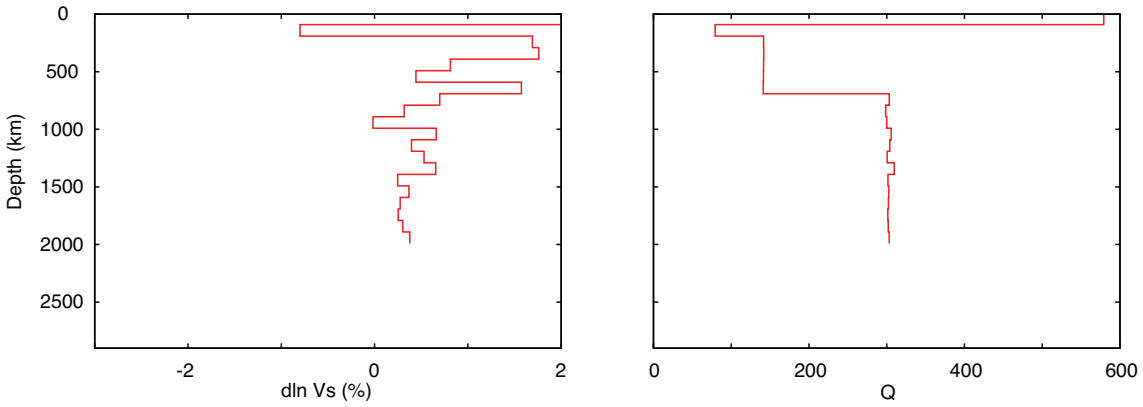

Figure S7. Models obtained with 1-D partial derivatives for shallower depth range.

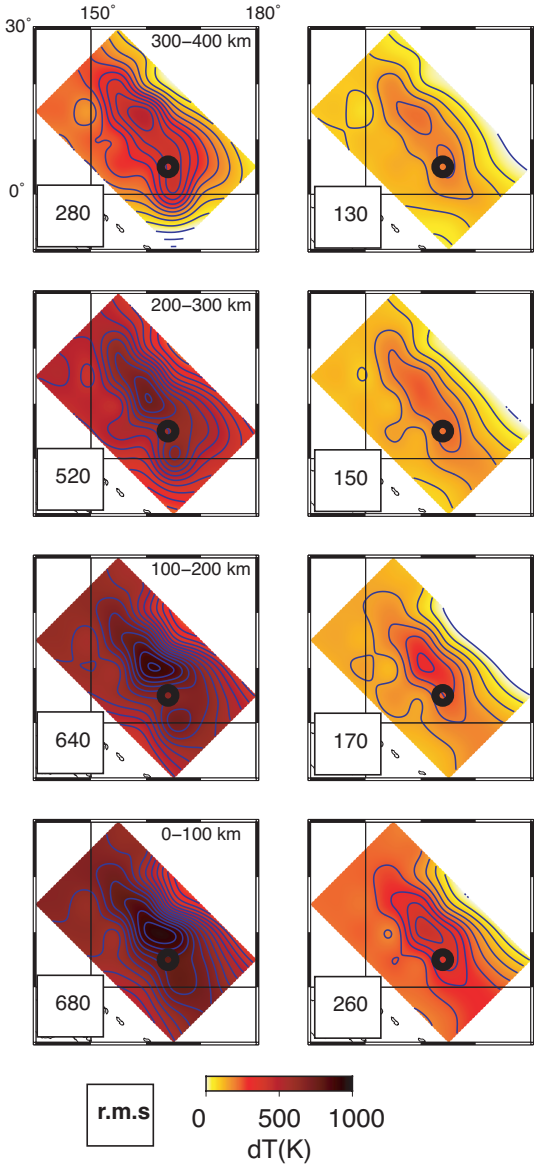

Figure S8. Temperature anomalies estimated from (a) $d \ln V_S$ and (b) dQ with smaller damping shown in Fig. 7. The contour interval is 50 K. In the right panels, depth range as expressed in distance from the CMB is provided at the top right. Insets at the bottom left of the panels show the root mean square (r.m.s) value for each depth range.

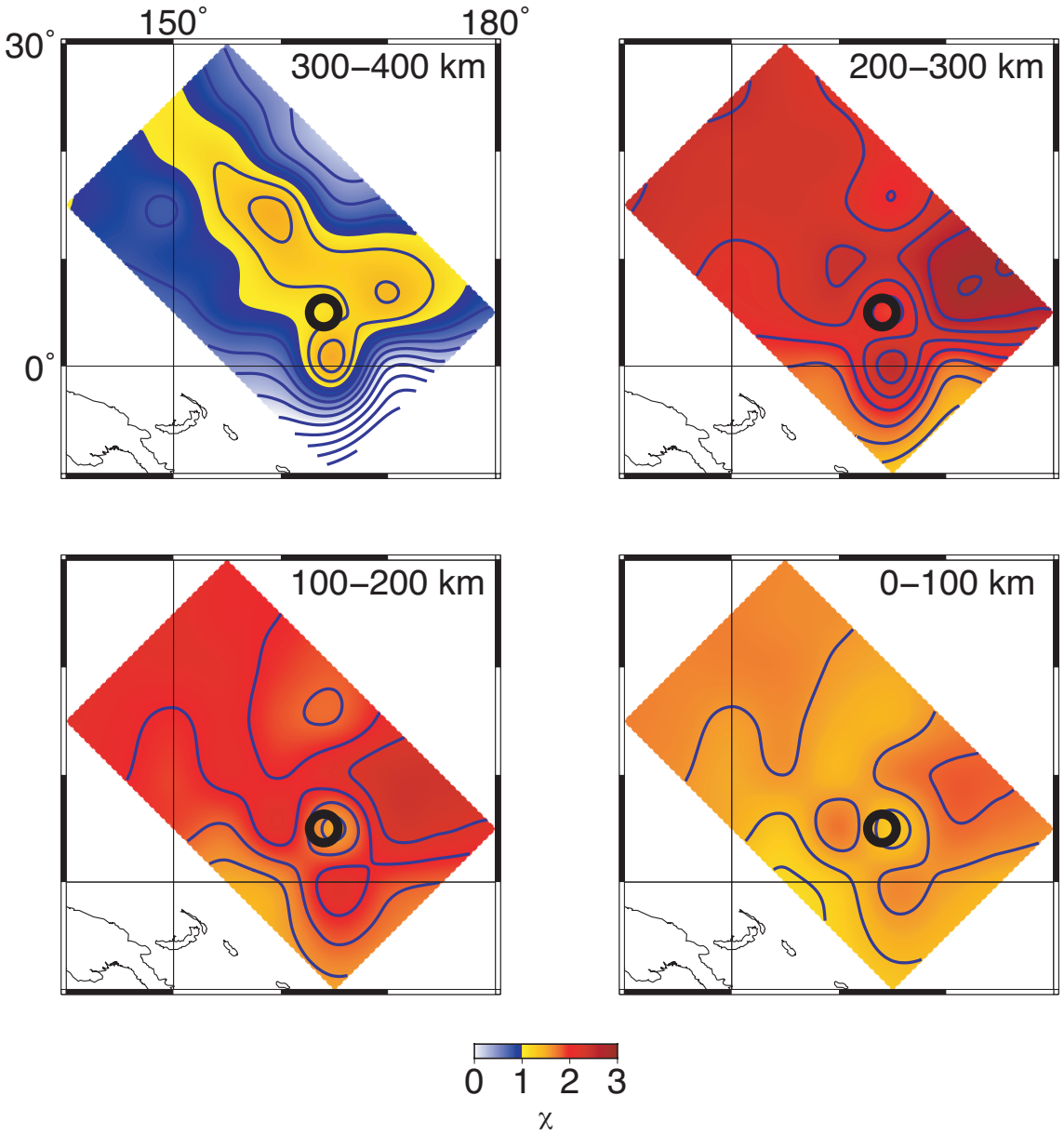

Figure S9. Distribution of the cost function χ for the models of dT_{V_S} and dT_Q obtained from the models of $d \ln V_S$ and Q with smaller damping plotted in Fig. 7. The contour interval is 0.2. Depth range as expressed in distance from the CMB is provided at the top right. Detailed in the text.

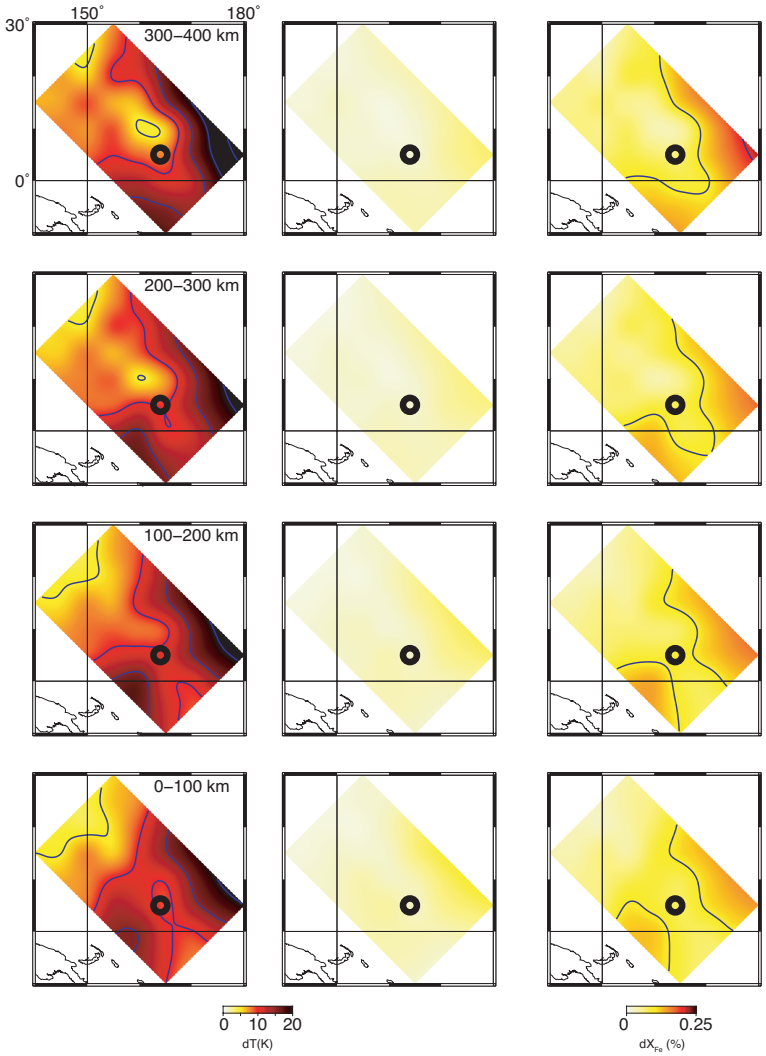

Figure S10. Differences between the temperature and chemical anomalies estimated from the $d\ln V_S$ and Q models obtained from the bootstrap test, and those obtained from our preferred model. The contour interval is 5 K and 0.1 % in dT and dFe, respectively.